Synthesis and Optical Characterization of Photoactive Poly(2-phenoxyethyl acrylate) Copolymers Containing Azobenzene Units, Prepared by Frontal Polymerization Using Novel Ionic Liquids as Initiators

Javier Illescas,[1,2] Yessica S. Ramirez-Fuentes,[1] Ernesto Rivera,[1] Omar G. Morales-Saavedra,[3] Antonio A. Rodríguez-Rosales,[3] Valeria Alzari,[2] Daniele Nuvoli,[2] Sergio Scognamillo,[2] Alberto Mariani[2]

[1]Instituto de Investigaciones en Materiales, Universidad Nacional Autónoma de México, Circuito Exterior S/N, Ciudad Universitaria, C.P. 04510 México D.F

[2]Dipartimento di Chimica, Università di Sassari, and Local INSTM Unit, Via Vienna 2, 07100 Sassari, Italy

[3]Centro de Ciencias Aplicadas y Desarrollo Tecnológico, Universidad Nacional Autónoma de México, Circuito Exterior S/N, Ciudad Universitaria, C.P. 04510 México D.F

Correspondence to: E. Rivera (E-mail: riverage@iim.unam.mx) or A. Mariani (E-mail: mariani@uniss.it)

ABSTRACT: 2-Phenoxyethyl acrylate (2-PEA) was polymerized alone and in the presence of an azobenzene comonomer derived from Disperse Red-1, N-ethyl-N-(2-hydroxyethyl)-4-(4-nitrophenylazo)aniline (MDR-1), by using the frontal polymerization technique. Two novel ionic liquids, recently synthesized by us, were used as initiators: tetrabutylphosphonium persulfate (TBPPS) and trihexyltetradecylphosphonium persulfate (TETDPPS). Even if their concentrations were smaller than those found when benzoyl peroxide and terbutylperoxy neodecanoate were used, these compounds gave rise to stable propagating polymerization fronts characterized by relatively low maximum temperatures and good velocities. Moreover, at variance to these latter, TBPPS and TETDPPS prevent bubble formation, thus allowing the use of the obtained materials in optical applications. The obtained polymers were characterized by infrared spectroscopy (FTIR), their thermal properties were determined by differential scanning calorimetry, and their optical properties were studied by absorption spectroscopy in the UV–vis region. Finally, the nonlinear optical (NLO) properties of the 2-PEA/MDR-1 copolymers obtained with TBPPS and TETDPPS were performed according to the Z-Scan technique with prepared film samples. It has been proven that samples with higher MDR-1 content (0.05 mol %) exhibited outstanding cubic NLO activity with negative NLO refractive coefficients around $n_2 = -1.7 \times 10^{-3}$ esu. © 2011 Wiley Periodicals, Inc. J Polym Sci Part A: Polym Chem 50: 821–830, 2012

KEYWORDS: azo polymers; frontal polymerization; NLO; poly(2-phenoxyethyl acrylate); radical polymerization

INTRODUCTION Frontal polymerization (FP) is a relatively easy technique that converts a mixture of monomer and initiator into polymer by means of an external stimulus, mainly thermal or photochemical.[1–5] This procedure offers some advantages compared with other polymerization methods and can also be applied in "green chemistry." Among these advantages, we can mention that: (a) no solvent is needed in the polymerization mixture, (b) because of the high temperatures reached by the fronts, FP generally guarantees reaction rates that are much larger than those found by using the classical polymerization techniques, and (c) there is a low energy consumption because the external energy source is applied only for the short time needed to ignite the polymerization reaction itself, whereas in a classical polymerization the energy source has to be maintained during the whole process.

Nowadays, FP has been used in many research fields and was first reported in 1972 by Chechilo et al. who carried out the polymerization of methyl methacrylate under high pressure conditions.[1] Since then, a considerable amount of research in this field has been developed. Our group used FP to synthesize hydrogels,[6–9] polymer-based nanocomposites,[10] unsaturated polyester/styrene resins,[11,12] nanocomposites containing polyhedral oligomeric silsesquioxanes,[13] interpenetrating polymer networks,[14] diurethane acrylates,[15] for the consolidation of tuff,[16] and to obtain polyurethanes.[17,18] In our most recent articles, we used FP to copolymerize successfully an azo monomer with an acrylic monomer,[19] to obtain stimuli-responsive hydrogels containing partially exfoliated graphite,[20] and to synthesize thermoresponsive super water absorbent hydrogels,[21] hybrid inorganic/organic epoxy resins.[22]

Pojman et al. studied the nonlinear behavior of the front,[23–26] the use of a microencapsulated initiator,[27,28] and the influence of the reactor geometry and the spin modes in the FP.[29] They reported the FP of poly(dicyclopentadiene),[30] simultaneous-interpenetrating polymer networks,[31] epoxy resins,[32] different acrylic monomers,[5,33–36] urethane-acrylates,[37] and ionic liquids.[38]

Chen et al. used the FP technique for the polymerization of N-methylolacrylamide,[39] vinylpyrrolidone,[40] polyurethane-nanosilica hybrid nanocomposites,[41] 2-hydroxyethyl acrylate,[42] quantum dot polymer nanocomposites,[43] and epoxy resin/polyurethane networks.[44] In their recent articles, FP was used as a method for the obtainment of colloidal crystal-loaded hydrogels[45] and fluorescent material-containing nanocomposites.[46] Moreover, they have reported a new class of FP, plasma-ignited FP for the preparation of hydrogels.[47] Other important studies in this research field have been done by Ivanov and Decker about the kinetic studies of the photoinitiated FP[48] and by Volpert and coworkers about the impact of the front velocity on frontal copolymerization.[49]

In a recent article, we demonstrated that the FP can be a technique exploitable to obtain materials that cannot be prepared by the classical method, namely, graphene-containing nanocomposite hydrogels of poly(N-isopropylacrylamide) were synthesized. At variance to what happened during the classical polymerization occurrence, because of the fast monomer into polymer conversion, graphene did not reaggregate to graphite flakes, thus allowing obtaining a homogeneously dispersed nanocomposite.[50]

Among the different kinds of monomers that might be able to undergo an FP process, a significant number of them were prepared for specific applications. However, not all the monomers can be polymerized using this technique. It depends on large measure on the physical and chemical properties of the monomer as well as on the selected initiator. The selected initiator is one of the most critical factors to be considered, because a huge amount of energy (heat), produced during the process, could cause bubble formation or monomer degradation as a result of the excessively high temperature reached by the front.

Recently, we reported the copolymerization of an azo monomer derived from Disperse Red-1 (DR-1), N-ethyl-N-(2-hydroxyethyl)-4-(4-nitrophenylazo)aniline (MDR-1), with poly(ethylene glycol) diacrylate (PEGDA) via FP.[19] Small amounts of this azo monomer provided outstanding optical properties to the obtained copolymer, because it changes its morphology and the orientation of the azobenzene groups after irradiation with UV light.

In this work, the feasibility of the FP of ethylene glycol phenyl ether acrylate (named also 2-phenoxyethyl acrylate, 2-PEA) was investigated. This is a hydrophobic monomer which confers solubility and wetting properties for adhesion or pigment carrying applications. 2-PEA monomer can form copolymers with acrylic or methacrylic acids and their salts, amides, esters, vinyl acetate, and styrene. In addition, their copolymers show excellent abrasion and resistance to polar solvents. Moreover, 2-PEA is mainly used in the elaboration of coatings for glass, metal, paper, plastic, wood, and PVC floor.[51,52]

Azo polymers have been considered as highly versatile materials because of the photoinduced motions that occur on them when they are irradiated with laser polarized light.[53] Many applications of azo polymers include waveguides, photolithography, and optical storage. Besides, these polymers exhibit nonlinear optical (NLO) properties of second- and third-harmonic generations, which make them attractive prospects for the elaboration of several optoelectronic devices.

Several reviews covering most of the implications of azobenzene in polymer structures have been published.[53–56] Rivera et al. have synthesized and characterized various azo polymers bearing amino-nitro-substituted azobenzene units.[57–60] In general, they exhibit maxima absorption wavelengths close to those reported for similar push-pull azo compounds.[61,62] In these materials, both H- and J-type aggregations have been observed in cast films.[58] This phenomenon can be used for optoelectronic and photonic applications, particularly photolithography and optical storage.

However, azo monomers usually exhibit slightly lower reactivity toward polymerization than acrylic and methacrylic monomers without azobenzene. It was previously reported that very often the homopolymerization of azo monomers gives polymers with medium to low molecular weights.[63] In some cases, when a radical initiator decomposes during the polymerization process a certain amount of undesirable gaseous by-products is produced. This is inconvenient for FP applications, because bubbled or porous materials, useless for most practical applications, can be obtained. Therefore, the choice of an appropriate initiator has to be seriously taken into account to avoid this problem. On the basis of a previous work by Pojman and coworkers,[64] Mariani et al. have reported the synthesis of two efficient ionic liquid radical initiators useful for this purpose, namely tetrabutylphosphonium persulfate (TBPPS) and trihexyltetradecylphosphonium persulfate (TETDPPS).[65]

Ionic liquids are organic or inorganic–organic salts, which are liquid at relatively low temperatures. Some of their most important characteristics can be listed as follows: (a) they are composed of poorly coordinating ions, (b) they are neither flammable nor explosive, (c) they are nonvolatile, and (d) they are compatible with most of the organic and inorganic compounds.

For these reasons, in this work, the FP technique has been used to copolymerize 2-PEA (which gave rise to the polymer matrix) with MDR-1 using TBPPS and TETDPPS as initiators. To compare the obtained results, besides 2-PEA, we used another matrix previously studied by us,[19] PEGDA, with the same ionic liquids. The structures of MDR-1, PEGDA, and 2-PEA are illustrated in Scheme 1.

The main scopes of this work are as follows: (1) to demonstrate that with the use of ionic liquids an amount of
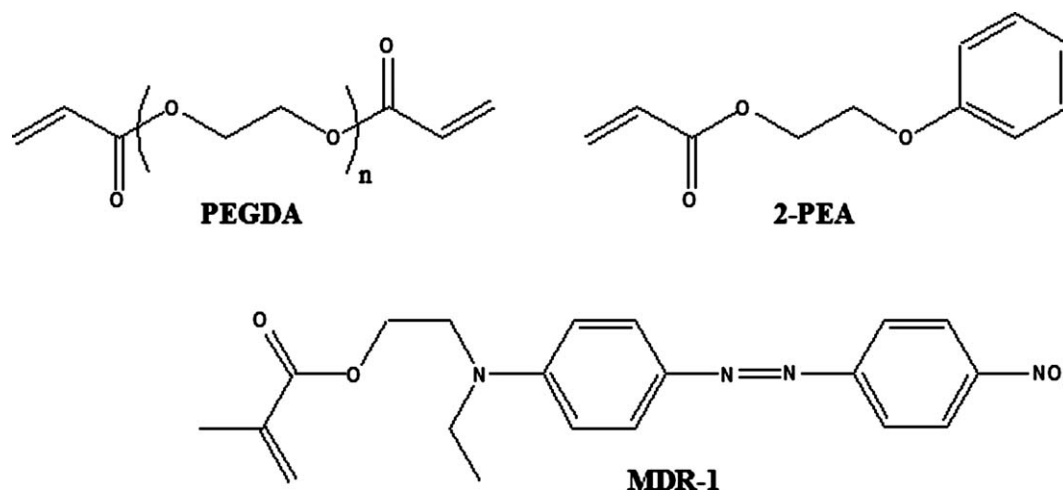
SCHEME 1 Structure of the used monomers.

initiator that is lower than that usually used in FP is required; (2) to copolymerize 2-PEA in the presence of an azo comonomer (MDR-1) to obtain samples with NLO response; and (3) to compare the efficiency of both ionic liquids (TBPPS and TETDPPS) in the FP of 2-PEA in the presence of MDR-1.

For this purpose, we carried out our experiments using different monomer/initiator ratios. Similarly, for the incorporation of MDR-1, we varied its concentration until the front was not able to propagate. For both sets of results, we determined the velocity of the front and its maximum temperature. The obtained polymer samples were characterized by FTIR spectroscopy, and their thermal properties were measured by differential scanning calorimetry (DSC). Moreover, the optical properties of these materials were studied by absorption spectroscopy in the solid state in the UV–vis range. Finally, the cubic NLO characterizations of the 2-PEA/MDR-1 amorphous copolymers, obtained with TBPPS and TETDPPS as initiators, were performed according to the Z-Scan technique in prepared film samples.

RESULTS AND DISCUSSION

Some preliminary FP experiments of 2-PEA were carried out with various initiators, and the results are summarized in Table 1, in which the minimum concentrations necessary for the front to self-sustain are reported. Even if benzoyl peroxide (BPO) and terbutylperoxy neodecanoate (Trigonox-23, T-23) gave rise to polymerization fronts, these latter were characterized by a large amount of bubbles because of the formation of volatile compounds as a result of both their degradation and high front temperature (ca. 190 °C). Because one of the final goals of this work was that of obtaining materials to be used in NLO applications, the presence of small bubbles embedded into the polymer matrix should be completely avoided. For such a reason, further studies on the use of the above mentioned initiators were abandoned.

The use of the ionic liquids TBPPS and TETDPPS as radical initiators allowed obtaining completely bubble-free polymer materials. Besides, to start the FP, they were required in a concentration that is much lower than that used with typical initiators. It is also worth mentioning that the maximum temperatures reached by using TETDPPS and TBPPS were significantly lower than those found with BPO and T-23 (142–152 °C). As a consequence, front velocities were almost halved (0.54–0.74 instead of 1.10–1.65 cm min^{-1}) but remaining within ranges that are still very interesting for practical optical applications such as NLO. It should be highlighted that with these last initiators the resulting polymers were completely transparent and did not contain any bubbles. Furthermore, conversions were always almost quantitative, leading to values ranging from 90 to 99% (Table 2).

Although with both ionic liquids the FP has been successfully achieved, there were significant differences in the results (Table 2). In detail, in the case of TBPPS, the conversion percentage diminished when the initiator content increased. As it was mentioned above, front velocity and maximum temperature values show an increase. Moreover, the glass transition temperature (T_g) remained almost constant between 12 and 14 °C. TETDPPS initiator was required in lower quantity than TBPPS to promote the formation of a propagating front.

TABLE 1 V_f, T_{max}, T_g, and Conversion for the FP of 2-PEA Using Various Initiators

Initiator	mol %	V_f (cm min^{-1})	T_{max} (°C)	T_g (°C)	Conversion (%)
BPO	0.79	1.10	193	ND	ND
T-23	1.29	1.65	189	ND	ND
TBPPS	0.068	0.74	152	14	98
TETDPPS	0.04	0.54	142	7	90

Only minimum concentrations allowing fronts to self-sustain are reported.
ND, not determined.

TABLE 2 V_f, T_{max}, T_g, and Conversion for the FP of 2-PEA Varying TBPPS or TETDPPS Initiator Concentration

Sample	Initiator (mol %)	V_f (cm min^{-1})	T_{max} (°C)	T_g (°C)	Conversion (%)
TBPPS					
B01	0.068	0.74	152	14	98
B02	0.14	1.19	175	13	97
B03	0.27	1.65	184	13	96
B04	0.54	2.27	195	12	94
B05	0.81	2.75	200	12	92
TETDPPS					
E01	0.04	0.54	142	7	90
E02	0.08	0.97	166	10	95
E03	0.16	1.27	178	12	96
E04	0.32	1.63	188	12	99
E05	0.41	1.98	191	9	99

TABLE 3 V_f, T_{max}, T_g, and Conversion for the FP of PEGDA Varying TBPPS or TETDPPS Initiator Concentration

Sample	Initiator (mol %)	V_f (cm min^{-1})	T_{max} (°C)	T_g (°C)	Conversion (%)
TBPPS					
001	0.2	0.44	125	−28	97
002	0.4	0.75	144	−27	78
003	0.8	1.16	155	−21	94
004	1.6	1.30	157	−20	96
005	2.4	1.00	150	−29	88
TETDPPS					
006	0.5	0.46	133	−29	94
007	1.0	0.72	141	−28	88
008	1.5	0.87	149	−25	88
009	2.5	1.12	154	−27	88

However, the most significant difference in efficiency between both initiators was the conversion; in particular, in the case of TETDPPS, this value increased within its concentration. Finally, it is worth to point out that this initiator exhibited an apparent antiplasticizer effect if compared with TBPPS. Indeed, the T_g values of the samples obtained with TETDPPS are generally a few degrees lower than those found for the samples prepared by using TBPPS.

To get further evidence about the efficiency of TBPPS and TETDPPS as initiators, we performed the FP of PEGDA, a monomer previously polymerized by us.[19] The results are summarized in Table 3. In this case, the obtained results confirmed the same trends found in the FP of 2-PEA; lower amounts of initiators were required and no bubble formation was observed during the FP process. In addition, front velocity and maximum temperature values increased as the initiator concentration increased.

The results for the copolymerization of 2-PEA with MDR-1, using TBPPS and TETDPPS, are shown in Table 4. As expected, front velocities, maximum temperatures, glass transition temperatures, and conversions diminished as the MDR-1 increased, which might be attributed to the slightly lower reactivity of the azo monomer toward radical polymerization. Indeed, there was a decrease in the conversion when TBPPS was used as initiator as the azo comonomer content was increased.

In contrast, TETDPPS gave practically an almost constant conversion value at different MDR-1 concentrations. These results suggest that TETDPPS is an initiator more efficient than TBPPS for the FP of 2-PEA. For such a reason, the characterization data here reported only refer to the copolymers prepared by using TETDPPS.

The thermal properties of the obtained polymers were evaluated by DSC. As it was previously mentioned, the conversion was almost quantitative and was determined by the following equation:

$$(\%) = [1 - (\Delta H_r/\Delta H_t)] \cdot 100,$$

where ΔH_r (residual) is the peak area obtained for the residual polymerization occurred during the first thermal scan, and ΔH_t (total) is the area under the curve when the polymerization was carried out in the DSC instrument. The conversion value for the copolymer of 2-PEA/MDR-1 with the highest azo monomer content (0.05 mol %) was estimated to be 94%. Moreover, a T_g value of 0 °C was found out from the second thermal scan of this copolymer.

The FTIR spectra of MDR-1 monomer and the polymers are shown in Figure 1. The characteristic bands of the MDR-1

TABLE 4 V_f, T_{max}, T_g, and Conversion for the FP of 2-PEA with MDR-1 and TBPPS (0.068 mol %) or TETDPPS (0.04 mol %) as Initiator

Sample	MDR-1 (mol %)	V_f (cm min^{-1})	T_{max} (°C)	T_g (°C)	Conversion (%)
TBPPS (0.068 mol %)					
BM01	0	0.74	152	14	96
BM02	0.005	0.78	154	10	96
BM03	0.013	0.72	151	9	93
BM04	0.025	0.73	149	10	95
BM05	0.050	0.58	144	3	88
BM06	0.130	ND	ND	ND	ND
TETDPPS (0.04 mol %)					
EM01	0	0.54	142	7	90
EM02	0.005	0.69	154	12	96
EM03	0.013	0.62	147	0	94
EM04	0.025	0.58	143	1	95
EM05	0.050	0.59	141	0	94
EM06	0.130	ND	ND	ND	ND

ND: Not determined because the polymerization process produces bubbled samples.
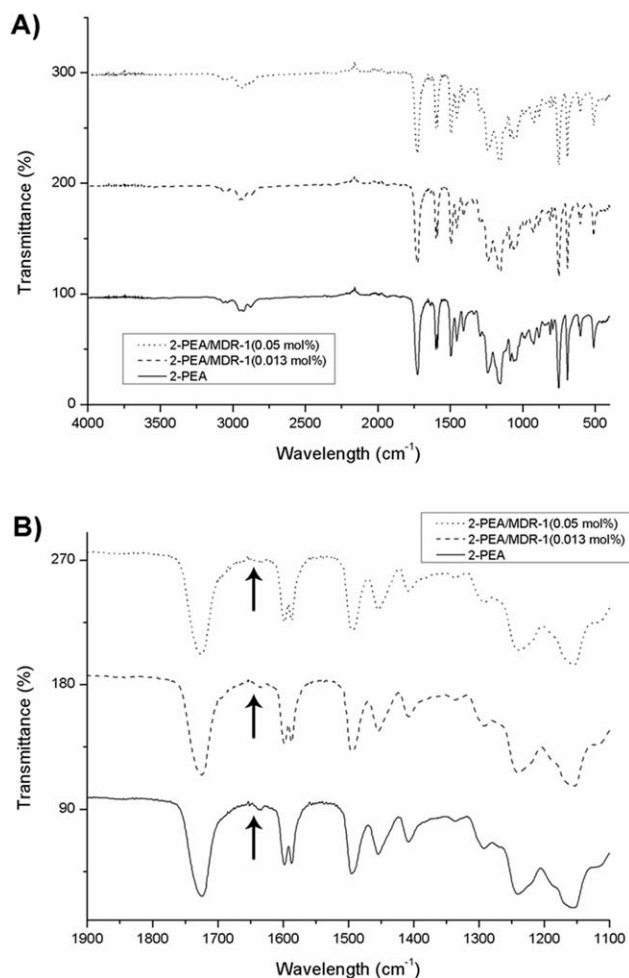
FIGURE 1 (a) FTIR analysis of 2-PEA polymer matrix and the copolymers with different MDR-1 concentrations (0.013 and 0.05 mol %; TETDPPS = 0.5 mol %). (b) For better analysis, an amplification of the FTIR spectra of the 2-PEA/MDR-1 copolymers is also included.

are indicated in the Experimental section. As we can see, the FTIR spectrum of the 2-PEA matrix exhibits a series of bands at $v = 2,896$ (s, CH$_2$), 1,743 (s, C=O), 1,267 (s, C—O esther), and 1,116 (s, O—CH$_2$) cm^{-1}.

The FTIR spectra of 2-PEA/MDR-1 copolymers with different azobenzene contents were recorded. If we analyze the spectrum of the 2-PEA/MDR-1 (0.05 mol % MDR-1 concentration) copolymer, we can observe a series of bands at 2,910 (s, CH$_2$, CH$_3$), 1,741 (s, C=O), 1,652 (s, C=C aromatic), 1,268 (s, C—O esther), and 1,120 (s, O—CH$_2$) cm^{-1}. Because the MDR-1 content is very low with respect to that of 2-PEA in the copolymers, it is very difficult to visualize the bands corresponding to the amino (R$_2$N), nitro (NO$_2$), and azo (N=N) groups. However, the presence of a broadening of the band at 1,625 cm^{-1}, due to the phenyl rings of the azobenzene moieties, which was not observed in the FTIR spectrum of the 2-PEA polymer, confirms that the azobenzene monomer was successfully incorporated into the copolymer.

The optical properties of the obtained polymers with TETDPPS as initiator were studied by UV–vis spectroscopy, and the absorption spectra of the copolymer bearing the highest MDR-1 content (0.05 mol %) are shown in Figure 2. As it could be expected, all copolymers (not shown) exhibited a maximum absorption band around 470–480 nm, whose intensity increases within the azobenzene content. To get a deeper insight in the optical properties of the polymers, we compared the absorption spectrum of the 2-PEA/MDR-1 (0.05 mol %) with those of the MDR-1 monomer and the oligomer isolated during the Soxhlet extraction. As we can see, the absorption spectrum of the MDR-1 monomer in CHCl$_3$ solution shows a well-defined maximum absorption band at $\lambda_{max} = 472$ nm as other amino-nitro-substituted azobenzenes do. This kind of azobenzene, which belong to the "pseudostilbenes" category, exhibits a total overlap of the π–π* and n–π* bands, which are inverted in the energy scale.[57] Similarly, the oligomer exhibited a well-defined band at $\lambda_{max} = 468$ nm, which is 4-nm blue shifted with respect to that of MDR-1, confirming the absence of remaining monomer during the FP process. This slight hypsochromic effect may be due to the slight presence of H-aggregation between the azobenzene groups in the oligomer. Further ^{1}H NMR experiments confirmed that such oligomer possesses relatively high azobenzene content.

On the other hand, the 2-PEA/MDR-1 (0.05 mol %) copolymer exhibited a broad absorption band centered at $\lambda_{max} = 482$ nm, which is 10-nm red shifted compared with that of MDR-1. However, the presence of an additional blue shifted shoulder at 432 nm, as well as the presence of a red shifted shoulder at 510 nm, reveals the presence of H-aggregates (antiparallel interactions) and traces of J-aggregates (head to tail interactions), respectively. It is very well known that polymers bearing donor-acceptor-substituted azobenzenes tend to form antiparallel pairs to reach certain neutrality and stability. This behavior was previously reported in the literature for other azo polymers.[63] According to the UV–vis spectra shown in Figure 2, the 2-PEA/MDR-1 (0.05 mol %)
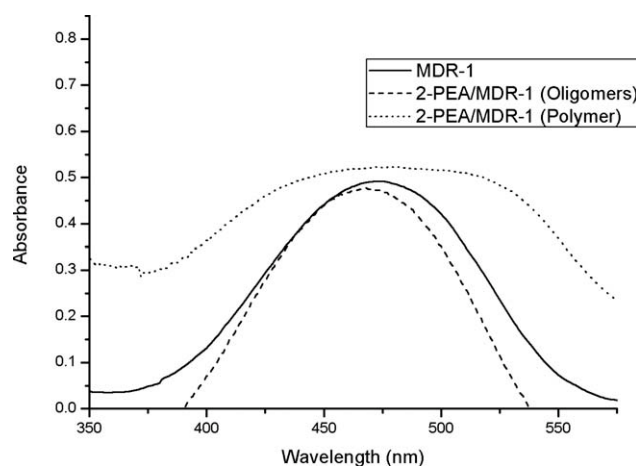

FIGURE 2 UV–vis spectra of the azo monomer MDR-1, the soluble oligomers, and the copolymer 2-PEA/MDR-1 with the highest azo monomer concentration (0.05 mol %; TETDPPS = 0.5 mol %).
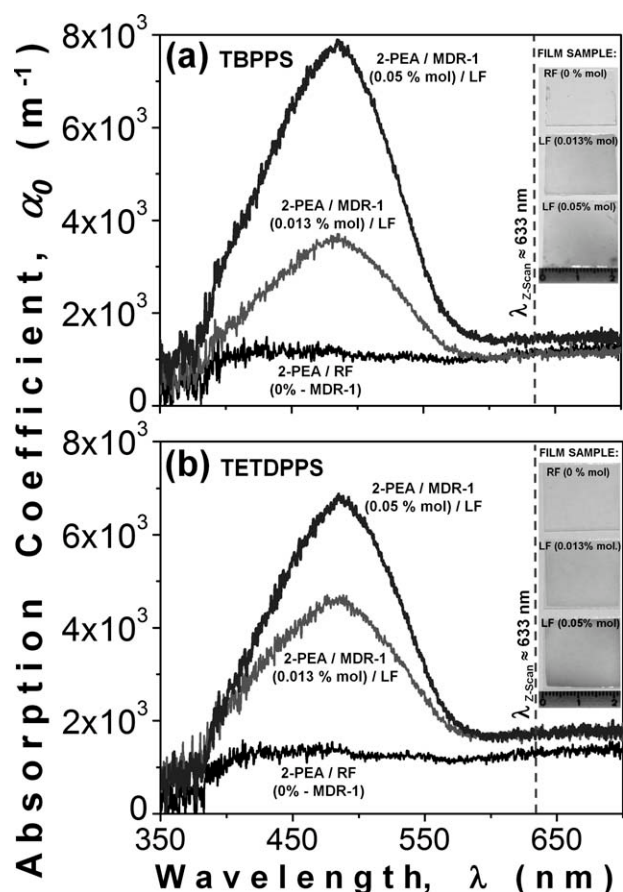
FIGURE 3 Comparative linear absorption coefficients obtained for the pristine 2-PEA reference films (RFs) and the 2-PEA/MDR-1 copolymer film samples (labeled films: LFs) prepared at different MDR-1 chromophore concentrations: (a) 2-PEA/MDR-1 copolymer film samples prepared with the TBPPS ionic liquid initiator and (b) 2-PEA/MDR-1 copolymer film samples prepared with the TETDPPS ionic liquid initiator.

copolymer shows the presence of H- and J-aggregates, which were not observed for the MDR-1 monomer.

Moreover, the linear absorption coefficients evaluated within the visible range for the 2-PEA/MDR-1 copolymer film sam-

ples with different MDR-1 chromophore contents (0.013 and 0.05 mol %) are shown in Figure 3. The thickness of the studied samples (sandwiched 2-PEA/MDR-1-labeled films prepared within two glass slices) was on the order of $\sim$80 μm (see values in Table 5). Thus, the Lambert–Beer law applies for such semitransparent film structures, allowing an adequate data analysis and making these copolymers potential candidates for some optical applications because of its appropriate transparency at optical wavelengths. From Figure 3, it is evident that the highest absorption of the samples occurs within the 380–580 nm spectral range in both 2-PEA/MDR-1 copolymers (the corresponding 2-PEA reference films do not exhibit significant absorption within the same spectral range). This fact confirms again the successful incorporation of the MDR-1 units into the 2-PEA polymeric matrix using the TBPPS and TETDPPS initiators. This fact points to additional conjugation of delocalized π-electrons provided by the higher content of azobenzene chromophores contained within these copolymer systems. This assumption will be explored by means of cubic NLO Z-Scan experiments as explained below. Under this framework, the available laser excitation line for Z-Scan experiments ($\lambda_{Z\text{-Scan}} = 632.8$ nm) is also depicted in this figure (vertical dashed line). At this wavelength, lowest absorption conditions occur, allowing nonresonant NLO characterizations of the developed film samples, which are a critical point when working with low T_g-based organic materials. In fact, relatively small linear absorption coefficients in the order of $\alpha_0 \approx 1200$–1800 m^{-1} (see values in Table 5) were evaluated for the studied copolymer films at $\lambda_{Z\text{-Scan}}$. These values are very useful for the determination of the nonlinear refraction and absorption coefficients according to the Z-Scan technique, as explained below.

Finally, the NLO Z-Scan measurements were performed at room conditions on the same 2-PEA/MDR-1 film samples (measurements include the reference 2-PEA-based films to monitor the NLO activity of the polymer matrix). The observed nonlocal effect of these samples is shown in Figure 4. A rigorous theoretical fitting was performed to simultaneously evaluate both the nonlinear absorptive and refractive properties of the studied copolymers. The NLO response of

TABLE 5 Structural, Linear, and Cubic NLO Parameters of the TBPPS- and TETDPPS-Based 2-PEA/MDR-1 Copolymer Films Measured According to UV–Vis Spectroscopy and the Z-Scan Technique

Film Sample (Ionic Liquid Initiator)	2-PEA:MDR-1 Concentration (mol %)	Film Thickness (μm)	Linear Absorption Coefficient: α_0 at $\lambda = 632.8$ nm (m^{-1})	$\Delta\phi_0/\Delta\psi_0$	NLO—Refractive Index: γ/n_2 Z-Scan at $\lambda = 632.8$ nm $\times 10^{-10}$ (m^2 W^{-1})/$\times 10^{-3}$ esu	NLO—Absorption Coefficient: β (TPA or SA) ($\times 10^{-4}$m W^{-1})
2-PEA/RF (TBPPS)	100:0.00	84	1240.70	−1.12/−0.02	−3.39/−1.27	−1.20 (SA)
2-PEA/MDR-1/LF (TBPPS)	100:0.05	82	1541.70	−1.50/−0.16	−4.65/−1.74	−9.84 (SA)
2-PEA/RF (TETDPPS)	100:0.00	90	1250.60	−0.98/−0.02	−2.66/−1.01	−1.11 (SA)
2-PEA/MDR-1/LF (TETDPPS)	100:0.05	88	1836.30	−1.05/0.00	−3.45/−1.30	0.00

Closed aperture Z-Scan measurements, at $\lambda_{Z\text{-Scan}} \approx 633$ nm, $S \approx 21\%$, Rayleigh range: $z_0 \approx 3.1$ mm.
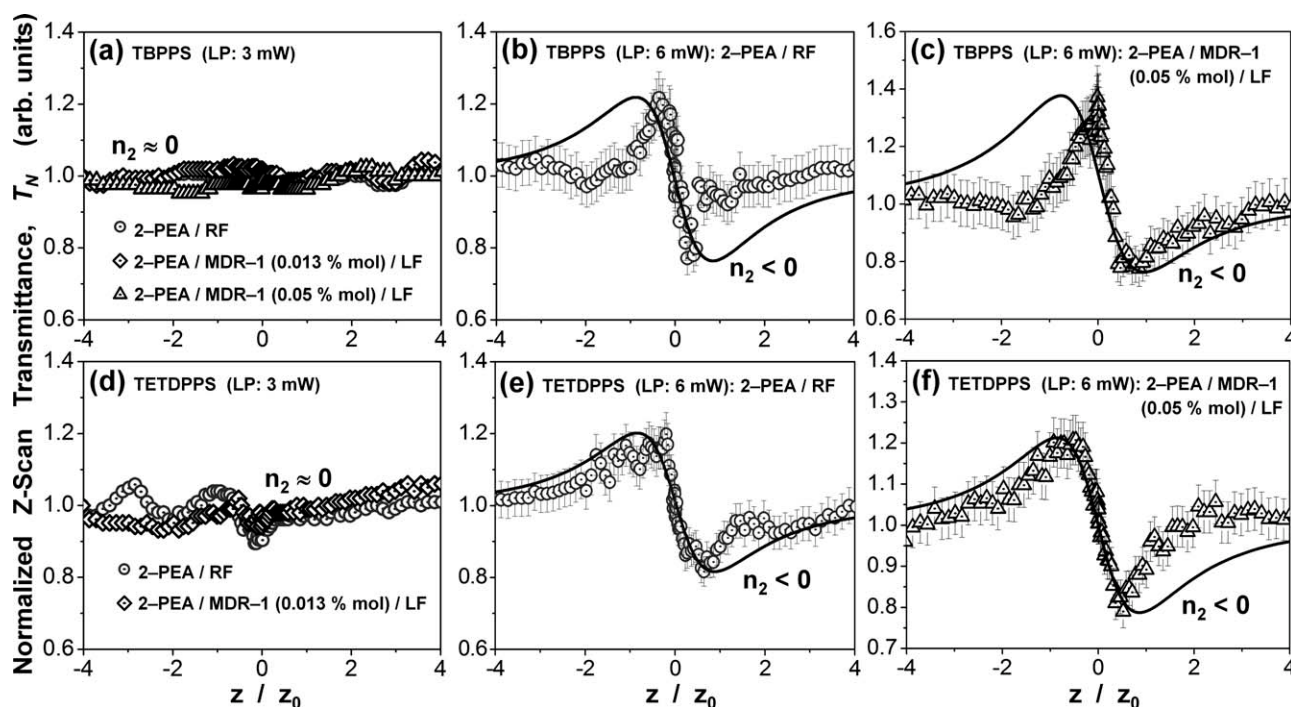
FIGURE 4 Closed aperture Z-Scan data (scattered points) and theoretical fitting (continuous lines) obtained at different laser powers (LP: 3 and 6 mW, at $\lambda_{Z\text{-Scan}}$ = 632.8 nm) and at different MDR-1 chromophore content for the TBPPS- and TETDPPS-based 2-PEA/MDR-1 copolymer/labeled films (LFs) and corresponding 2-PEA reference films (RFs): (a–c) TBPPS-based film samples and (d–f) TETDPPS-based film samples. An estimated experimental error below 6% is also considered for the Z-Scan data (error bars).

the developed films was characterized by varying the polarization input planes of the He-Ne laser system to explore microscopic material asymmetries or anisotropies throughout the sample structure (measurements were also performed on several regions of the specimens to verify the experimental results). In general, because all NLO measurements were systematically performed with different laser input polarization states (from 0° to 90°: s- and p-polarization, respectively) and the obtained curves are quite similar in each sample, the film structures do not seem to show any significant anisotropic behavior, thus confirming their amorphous nature. On the other hand, because all the studied samples have relatively low glass transition temperature values (T_g around 10 °C), the Z-Scan curves and related NLO effects were only obtained at low laser intensity threshold values. Indeed, Z-Scan measurements performed on the highly transparent 2-PEA reference films and on the corresponding 2-PEA/MDR-1 film samples (labeled films: LFs) exhibit negligible nonlinear refraction and absorption effects for laser powers below 6 mW [$n_2 \approx 0$, see Fig. 4(a,d)]. At a LP ≈ 6 mW, the cubic NLO properties of the samples become evident. Taking into account the theory developed by Sheik-Bahae et al. and Liu et al.,[66–70] it is observed from our measurements that the nonlinear refractive response of the studied samples can be unambiguously determined by typical peak-to-valley transmittance curves. Hence, one can immediately observe that the pristine 2-PEA reference films exhibit non-negligible negative NLO refractive properties at this laser power regime [$n_2 < 0$, see Fig. 4(b,e)]. Furthermore,

the corresponding 2-PEA/MDR-1 films [at higher MDR-1 content: 0.05 mol %, see Fig. 4(c,f)] exhibit stronger NLO refractive coefficients (see Table 5). Given that the glass slices implemented to sandwich the copolymer films do not contribute to the NLO effects at the implemented low laser powers (Z-Scan curves not shown here for clearness in the curves), it is indeed assumed that the increase of the NLO response of the samples is promoted by a successful copolymerization of the NLO-active MDR-1 comonomer with the 2-PEA matrix comonomer. As previously discussed, the copolymerization process is more efficient when implementing the TETDPPS ionic liquid initiator to form the 2-PEA/MDR-1 copolymers; this fact was also sensitively detected via NLO measurements as the corresponding theoretical fits (TFs) are better correlated to the experimental data, indicating a more stable and homogeneous copolymer film sample.

The respective TFs to the obtained Z-Scan transmission data (solid lines) are also shown in Figure 4(a–f). To perform the TFs according to previous theoretical studies, the normalized Z-Scan transmittance T_N can be determined as a function of the dimensionless sample position ($x = z/z_0$), where z_0 is the Rayleigh range and z is the Z-Scan sample position (laboratory reference frame). Hence, the TFs were obtained according to the following equation, considering both nonlinear refraction and absorption effects.[66]

$$T_N \approx 1 + \left[4x/(1+x^2)(9+x^2)\right]\Delta\Phi$$
$$- \left[2(x^2+3)/(1+x^2)(9+x^2)\right]\Delta\Psi. \quad (1)$$

Here, the second term is related to NLO refractive effects, whereas the third one is associated with NLO absorptive phenomena (the first term is a normalization factor). Indeed, because the obtained Z-Scan data clearly exhibit a peak-to-valley transmittance asymmetry, NLO absorption effects are also expected.[66] The fitting parameters are, in this case, the induced phase shifts $\Delta\Phi$ or $\Delta\Psi$, respectively. In the former case, the phase shift is given by: $\Delta\Phi = 2\pi\gamma I_0 L_{\text{eff}}/\lambda$,[66] from which the NLO refractive index (n_2- or γ-coefficient) can be obtained. In the latter case, the phase shift is provoked by the NLO absorptive phenomena and is given by $\Delta\Psi = \beta I_0 L_{\text{eff}}/2$,[66] allowing the evaluation of the NLO absorption (β-coefficient), either due to two photon (or multiphoton) absorption and/or saturable absorption. In these equations, λ is the laser wavelength, I_0 is the input beam intensity (at focal spot: $z = 0$), and L_{eff} is the effective thickness of the film sample, defined as: $L_{\text{eff}} = [1 - (e^{-\alpha_0 L_S})](\alpha_0)^{-1}$, where α_0 represents the linear absorption coefficient. All these equations are well established and have been proven in early Z-Scan works.[66–71] The theoretical restrictions imposed by these formulas to apply such expressions at optimal conditions ($|\Delta\Phi_0| < \pi$, $S \approx 20\%$, etc.) are not always fully satisfied in our experimental result because of the large phase shifts and huge nonlinearities obtained in our experiments. Nevertheless, in most cases (mainly in the case of well-defined $\gamma > 0$ or $\gamma < 0$ curves), our results nearly satisfy these conditions and can be conveniently fitted according to these theoretical formulas. Thus, for comparison purposes and to be consistent with the estimation of the γ- and β-values, we assumed their applicability and used them in our experimental results. The TFs allowed us to evaluate largest negative NLO refractive coefficients in the order of $\gamma = -4.65 \times 10^{-10}$ m^2 W^{-1} (or $n_2 = -1.74 \times 10^{-3}$ esu) and a NLO absorption coefficient of $\beta = -9.84 \times 10^{-4}$ m W^{-1} (corresponding to the 2-PEA/MDR-1 film sample developed with the TBPPS ionic liquid initiator at higher MDR-1 content: 0.05 mol %). The obtained γ/n_2-values are very large, many orders of magnitude larger than those observed for typical glass substrates or for the classical CS$_2$ standard reference material: $+1.2 \times 10^{-11}$ esu (Z-Scan at $\lambda = 10.6$ μm) or 6.8×10^{-13} esu (DFWM at $\lambda = 532$ nm).[67–71] On the other hand, the negative sign obtained for the β-coefficients reveals the nature of the NLO absorptive phenomena of the samples, indicating strong saturable absorption (SA) effects.[67–71] This fact indicates convenient material properties to avoid undesired photothermal effects during Z-Scan experiments due to long continuous-wave laser irradiation and low T_g values of the samples. Indeed, Z-Scan experiments were performed at extremely low laser energy ($\sim$3 and 6 mW) to avoid photodegradation and reorientation effects on the sample, which inevitably started at laser power regimens in the order of around 10 mW.

EXPERIMENTAL

Materials

PEGDA ($M_n \cong 575$, $d = 1.12$ g mL^{-1}), 2-PEA (FW = 192.2, $d = 1.103$ g mL^{-1}), triethylamine (FW = 101.19, bp = 88.8 $^\circ$C, $d = 0.726$ g mL^{-1}), and DR-1 dye (FW = 314.34, mp = 160–162 $^\circ$C) were purchased from Sigma-Aldrich. Tetrabutyl-phosphonium chloride (FW = 294.89, mp = 62–66 $^\circ$C), tri-hexyltetradecylphosphonium chloride (FW = 519.31, $d = 0.895$ g mL^{-1}), BPO (FW = 242.23, mp = 102–105 $^\circ$C), and methacryloyl chloride (FW = 104.53, bp = 95–96 $^\circ$C, $d = 1.07$ g mL^{-1}) were purchased from Fluka. T-23 (FW = 244.4, $d = 0.916$ g mL^{-1}) was purchased from Akzo-Nobel. All reagents used in the polymer synthesis were used as received, without further purification.

The azo monomer derived from Disperse-Red 1 (MDR-1) and the ionic liquids TBPPS and TETDPPS were synthesized according to the procedures previously described in the literature.[19,65]

FP Experiments

FP runs were performed as follows: in a glass test tube (16-cm length, 16-mm diameter), a suitable amount of monomer (2-PEA or PEGDA), azo comonomer (MDR-1), and initiator (BPO or T-23 or TBPPS or TETDPPS) were placed without any solvent and mixed until all the initiator was completely dissolved.

The tubes containing the mixture were locally heated at the top level of the solution, using the tip of a soldering iron as the external heating source, until the formation of a propagating front was observed. The heat released during the conversion of the monomer into polymer was responsible for the formation of a hot front, able to self-sustain the polymerization process and the propagation throughout the whole tube. The polymerization was very fast and it took only a few minutes to be performed. Front velocity (± 0.05 cm min^{-1}) and front maximum temperature (± 10 $^\circ$C) were recorded.

Characterization

Temperature profiles were measured using a K-type thermocouple placed in the monomer–initiator mixture above 2 cm (± 0.5 cm) from the bottom of the tube. This thermocouple was connected to a digital thermometer (Delta Ohm 9416), which was used for temperature reading. The position of the front, easily visible through the glass walls of the tube, was measured as a function of the time.

Once the polymerizations were accomplished, the obtained samples were removed from tubes and analyzed by DSC to determine the conversion percentage. DSC measurements were conducted in a DSC Q100 Waters TA Instrument. For each sample, two consecutive scans were carried out under argon atmosphere from -80 to 300 $^\circ$C with a heating rate of 10 $^\circ$C min^{-1}; monomer conversion was determined from the first thermal scan, whereas T_g values were obtained from the second scan.

FTIR spectra of the samples were recorded in a Fourier transform infrared spectrometer (JASCOFT 480) in KBr pressed pellets. For each sample, 16 scans were recorded at a resolution of 4 cm^{-1}.

The UV–vis spectra of the azo monomer ($CHCl_3$ solution, 1-cm quartz cell) and the copolymers (solid state) were recorded in a Hitachi U-2010 spectrometer. This technique was useful to determine the MDR-1 content in all polymer samples. The extinction coefficient of the MDR-1 in $CHCl_3$ solution was estimated to be 46,700 M cm^{-1}.

At last, the resulting 2-PEA/MDR-1 copolymers were also studied in film samples as active media for cubic $\chi^{(3)}$-NLO effects such as nonlinear refraction and nonlinear absorption via the Z-Scan technique.[72] The experimental Z-Scan setup was implemented using an unpolarized laser beam from a 35-mW He-Ne laser system working at 632.8 nm (THORLABS, HRR170-1). Its energy was carefully monitored and kept constant during long Z-Scan measurements. The spatial mode of the laser beam was close to Gaussian TEM$_{00}$. The polarization plane of the He-Ne laser beam was adjusted and controlled by means of a linear polarizer mounted on a rotation stage. The polarized laser beam was focused on the sample by means of a positive lens ($f = 5$ cm), so that a light power density of $\sim 8.53 \times 10^6$ W m^{-2} reached the studied samples at the focal spot. At last, film samples were mounted on a motorized translation stage (25-mm length travel in steps of 2 μm) to perform Z-Scan experiments within the focal range. A large area Si-photodetector (EOT ET-2040) was located at ~ 0.96 m from the focusing lens, after a 2.5-mm diameter (20% transmittance) diaphragm aperture. All NLO signals captured from photodetectors were measured with a digital oscilloscope (Tektronix TDS, 744A), and all motion systems and Z-Scan setup management were automated via a LabView control program.

CONCLUSIONS

In this work, the frontal copolymerization of (E)-2-(ethyl(4-((4-nitrophenyl)diazenyl)phenyl)amino)ethyl methacrylate (MDR-1) with 2-PEA was carried out. The influence of the MDR-1 content and the type and amount of initiator were studied to determine the optimum concentration range in which FP can occur. The best results for the polymerization of 2-PEA were obtained with the ionic liquid TETDPPS. Indeed, even though with both TBPPS and TETDPPS homogeneous polymer samples (not bubbled) were obtained, a higher quantity of initiator was required when TBPPS was used. Moreover, with this latter, the maximum reached temperature was significantly higher. Azo polymers containing up to 0.05 mol % of MDR-1 were successfully prepared. Such concentration is good enough to confer them outstanding NLO properties. The UV–vis spectra of the obtained polymers exhibit a significant broadening of the absorption bands with blue- and red-shifted shoulders, because of the presence of H- and J-aggregates. Outstanding cubic NLO effects were measured via the Z-Scan technique in the developed 2-PEA/MDR-1 copolymer film samples with higher MDR-1 content (0.05 mol %), where negative NLO refractive coefficients in the order of 10^{-3} esu were found. The 2-PEA/MDR-1 films (obtained with TETDPPS) exhibited a more stable NLO behavior because the respective theoretical fittings were better correlated to the experimental data, indicating an optimal azobenzene incorporation into 2-PEA/MDR-1, when TETDPPS ionic liquid was used as initiator. In addition, the NLO absorptive response of these materials was established as a saturable absorption process, protecting the samples, at least to some extent, from photodegradation effects in spite of their low T_g values. However, more NLO studies should be performed on these materials to further understand the electronic and thermal contributions to the cubic nonlinearities. Additionally, complementary studies on the MDR-1 loading in these copolymers and other systems should also be performed to improve both the NLO response and thermal properties for stable NLO applications (including quadratic NLO effects in prepared electrically poled film samples).

REFERENCES AND NOTES

1 Chechilo, N. M.; Khvilivitskii, R. J.; Enikolopyan, N. S. *Dokl. Akad. Nauk. SSSR* **1972**, *204*, 1180–1181.

2 Chechilo, N. M.; Enikolopyan, N. S. *Dokl. Phys. Chem.* **1976**, *230*, 840–843.

3 Davtyan, S. P.; Surkov, N. F.; Rozenberg, B. A.; Enikolopyan, N. S. *Dokl. Phys. Chem.* **1977**, *32*, 64–67.

4 Davtyan, S. P.; Zhirkov, P. V.; Vol'fson, S. A. *Russ. Chem. Rev.* **1984**, *53*, 150–163.

5 Pojman, J. A. *J. Am. Chem. Soc.* **1991**, *113*, 6284–6286.

6 Caria, G.; Alzari, V.; Monticelli, O.; Nuvoli, D.; Kenny, J. M.; Mariani, A. *J. Polym. Sci. Part A: Polym. Chem.* **2009**, *47*, 1422–1428.

7 Gavini, E.; Mariani, A.; Rassu, G.; Bidali, S.; Spada, G.; Bonferoni, M. C.; Giunchedi, P. *Eur. Polym. J.* **2009**, *45*, 690–699.

8 Alzari, V.; Monticelli, O.; Nuvoli, D.; Kenny, J. M.; Mariani, A. *Biomacromolecules* **2009**, *10*, 2672–2677.

9 Scognamillo, S.; Alzari, V.; Nuvoli, D.; Mariani, A. *J. Polym. Sci. Part A: Polym. Chem.* **2010**, *48*, 2486–2490.

10 Mariani, A.; Bidali, S.; Caria, G.; Monticelli, O.; Russo, S, Kenny, J. M. *J. Polym. Sci. Part A: Polym. Chem.* **2007**, *45*, 2204–2212.

11 Fiori, S.; Mariani, A.; Bidali, S.; Malucelli, G. *e-Polymers* **2004**, *001*, 1–12.

12 Fiori, S.; Malucelli, G.; Mariani, A.; Ricco, L.; Casazza, E. *e-Polymers* **2002**, *057*, 1–10.

13 Mariani, A.; Alzari, V.; Monticelli, O.; Pojman, J. A.; Caria, G. *J. Polym. Sci. Part A: Polym. Chem.* **2007**, *45*, 4514–4521.

14 Fiori, S.; Mariani, A.; Ricco, L.; Russo, S. *e-Polymers* **2002**, *029*, 1–10.

15 Mariani, A.; Fiori, S.; Bidali, S.; Alzari, V.; Malucelli, G. *J. Polym. Sci. Part A: Polym. Chem.* **2008**, *46*, 3344–3352.

16 Mariani, A.; Bidali, S.; Cappelletti, P.; Caria, G.; Colella, A.; Brunetti, A.; Alzari, V. *e-Polymers* **2009**, *064*, 1–12.

17 Mariani, A.; Bidali, S.; Fiori, S.; Malucelli, G.; Sanna, E. *e-Polymers* **2003**, *044*, 1–9.

18 Fiori, S.; Mariani, A.; Ricco, L.; Russo, S. *Macromolecules* **2003**, *36*, 2674–2679.

19 Illescas, J.; Ramírez-Fuentes, Y. S.; Rivera, E.; Morales-Saavedra, O. G.; Rodríguez-Rosales, A. A.; Alzari, V.; Nuvoli, D.; Scognamillo, S.; Mariani, A. *J. Polym. Sci. Part A: Polym. Chem.* **2011,** *49*, 3291–3298.

20 Alzari, V.; Mariani, A.; Monticelli, O.; Valentini, L.; Nuvoli, D.; Piccinini, M.; Scognamillo, S.; Bittolo Bon, S.; Illescas, J. *J. Polym. Sci. Part A: Polym. Chem.* **2010,** *48*, 5375–5381.

21 Scognamillo, S.; Alzari, V.; Nuvoli, D.; Illescas, J.; Marceddu, S.; Mariani, A. *J. Polym. Sci. Part A: Polym. Chem.* **2011,** *49*, 1228–1234.

22 Scognamillo, S.; Alzari, V.; Nuvoli, D.; Mariani, A. *J. Polym. Sci. Part A: Polym. Chem.* **2010,** *48*, 4721–4725.

23 Pojman, J. A.; Ilyashenko, V. M.; Khan, A. M. *J. Chem. Soc. Faraday Trans.* **1996,** *92*, 2824–2836.

24 Ilyashenko, V. M.; Pojman, J. A. *Chaos* **1998,** *8*, 285–289.

25 Nagy, I. P.; Pojman, J. A. *J. Phys. Chem.* **1996,** *100*, 3299–3304.

26 Epstein, I. R.; Pojman, J. A. *Chaos* **1999,** *9*, 255–259.

27 McFarland, B.; Popwell, S.; Pojman, J. A. *Macromolecules* **2006,** *39*, 53–63.

28 McFarland, B.; Popwell, S.; Pojman, J. A. *Macromolecules* **2004,** *37*, 6670–6672.

29 Pojman, J. A.; Masere, J.; Pettreto, E.; Rustici, M.; Volpert, V. *Chaos* **2002,** *12*, 56–65.

30 Mariani, A.; Fiori, S.; Chekanov, Y.; Pojman, J. A. *Macromolecules* **2001,** *34*, 6539–6541.

31 Pojman, J. A.; Elcan, W.; Khan, A. M.; Mathias, L. *J. Polym. Sci. Part A: Polym. Chem.* **1997,** *35*, 227–230.

32 Chekanov, Y.; Arrington, D.; Brust, G.; Pojman, J. A. *J. Appl. Polym. Sci.* **1997,** *66*, 1209–1216.

33 Nason, C.; Roper, T.; Hoyle, C.; Pojman, J. A. *Macromolecules* **2005,** *38*, 5506–5512.

34 Khan, A. M.; Pojman, J. A. *Trends Polym. Sci.* **1996,** *4*, 253–257.

35 Fortenberry, D. I.; Pojman, J. A. *J. Polym. Sci. Part A: Polym. Chem.* **2000,** *38*, 1129–1135.

36 Nason, C.; Pojman, J. A.; Hoyle, C. *J. Polym. Sci. Part A: Polym. Chem.* **2008,** *46*, 8091–8096.

37 Pojman, J. A.; Chen, L. *J. Polym. Sci. Part A: Polym. Chem.* **2006,** *44*, 3018–3024.

38 Jimenez, Z.; Pojman, J. A. *J. Polym. Sci. Part A: Polym. Chem.* **2007,** *45*, 2745–2754.

39 Chen, L.; Hu, T.; Yu, H.; Chen, S.; Pojman, J. A. *J. Polym. Sci. Part A: Polym. Chem.* **2007,** *45*, 4322–4330.

40 Cai, X.; Chen, S.; Chen, L. *J. Polym. Sci. Part A: Polym. Chem.* **2008,** *46*, 2177–2185.

41 Chen, S.; Sui, J.; Chen, L.; Pojman, J. A. *J. Polym. Sci. Part A: Polym. Chem.* **2005,** *43*, 1670–1680.

42 Hu, T.; Chen, S.; Tian, Y.; Chen, L.; Pojman, J. A. *J. Polym. Sci. Part A: Polym. Chem.* **2007,** *45*, 873–881.

43 Fang, Y.; Chen, L.; Wang, C. F.; Chen, S. *J. Polym. Sci. Part A: Polym. Chem.* **2010,** *48*, 2170–2177.

44 Chen, S.; Tian, Y.; Chen, L.; Hu, T. *Chem. Mater.* **2006,** *18*, 2159–2163.

45 Liu, S. S.; Yu, Z. Y.; Fang, Y.; Yin, S. N.; Wang, C. F.; Chen, S. *J. Polym. Sci. Part A: Polym. Chem.* **2011,** *49*, 3121–3128.

46 Guo, X.; Wang, C. F.; Fang, Y.; Chen, L.; Chen, S. *J. Mater. Chem.* **2011,** *21*, 1124–1129.

47 Zhou, J.; Shao, H.; Tu, J.; Fang, Y.; Guo, X.; Wang, C. F.; Chen, L.; Chen, S. *Chem. Mater.* **2010,** *22*, 5653–5659.

48 Ivanov, V. V.; Decker, C. *Polym. Int.* **2001,** *50*, 113–118.

49 Perry, M. F.; Volpert, V. A.; Lewis, L. L.; Nichols, H. A.; Pojman, J. A. *Macromol. Theory Simul.* **2003,** *12*, 276–286.

50 Alzari, A.; Nuvoli, D.; Scognamillo, S.; Piccinini, M.; Gioffredi, E.; Malucelli, G.; Marceddu, S.; Sechi, M.; Sanna, V.; Mariani, A. *J. Mater. Chem.* **2011,** *21*, 8727–8733.

51 Bitkina, A. V.; Malkova, L. A.; Panchenko, S. V. *Labor Med. Ind. Ecol.* **1994,** *7*, 37–38.

52 Van Miller, J. P.; Garman, R. H.; Hermansky, S. J.; Mirsalis, J. C.; Frederick, C. B. *Reg. Toxicol. Pharmacol.* **2003,** *37*, 54–65.

53 Hu, X.; Zheng, P. J.; Zhao, X. Y.; Li, L.; Tam, K. C.; Gan, L. H. *Polymer* **2004,** *45*, 6219–6225.

54 Ikeda, T.; Ooya, T.; Yui, N. *Polym. J.* **1999,** *31*, 658–663.

55 Takashima, Y.; Nakayama, T.; Miyauchi, M.; Kawaguchi, Y. *Chem. Lett.* **2004,** *33*, 890–891.

56 Tung, C. H.; Wu, L. Z.; Zhang, L. P.; Chen, B. *Acc. Chem. Res.* **2003,** *36*, 39–47.

57 Rivera, E.; Belletête, M.; Natansohn, A.; Durocher, G. *Can. J. Chem.* **2003,** *81*, 1076–1082.

58 Rivera, E.; Carreón-Castro, M. P.; Salazar, R.; Huerta, G.; Becerril, C.; Rivera, L. *Polymer* **2007,** *48*, 3420–3428.

59 Rivera, E.; Carreón-Castro, M. P.; Buendía, I.; Cedillo, G. *Dyes Pigments* **2006,** *68*, 217–226.

60 Rivera, E.; Carreón-Castro, M. P.; Rodríguez, L.; Cedillo, G.; Fomine, S.; Morales-Saavedra, O. G. *Dyes Pigments* **2007,** *74*, 396–403.

61 Meng, X.; Natansohn, A.; Barrett, C.; Rochon, P. *Macromolecules* **1996,** *29*, 946–952.

62 Kasha, M. *Radiat. Res.* **1963,** *20*, 55–71.

63 Freiberg, S.; Lagugné-Labarthet, F.; Rochon, P.; Natansohn, A. *Macromolecules* **2003,** *36*, 2680–2688.

64 Masere, J.; Chekanov, Y.; Warren, J. R.; Stewart, F.; Al-Kaysi, R.; Rasmussen, J. K.; Pojman, J. A. *J. Polym. Sci. Part A: Polym. Chem.* **2000,** *38*, 3984–3990.

65 Mariani, A.; Nuvoli, D.; Alzari, V.; Pini, M. *Macromolecules* **2008,** *41*, 5191–5196.

66 Liu, X.; Guo, S.; Wang, H.; Hou, L. *Opt. Commun.* **2001,** *197*, 431–437.

67 Sheik-Bahae, M.; Said, A. A.; Van Stryland, E. W. *Opt. Lett.* **1989,** *14*, 955–957.

68 Sheik-Bahae, M.; Said, A. A.; Hagan, D. J.; Soileau, M. J.; Van Stryland, E. W. *Opt. Eng.* **1991,** *30/8*, 1228–1235.

69 Sheik-Bahae, M.; Said, A. A.; Wei, T. H.; Hagan, D. J.; Van Stryland, E. W. *IEEE J. Quant. Electron* **1990,** *26*, 760–769.

70 Xia, T.; Hagan, D. J.; Sheik-Bahae, M.; Van Stryland, E. W. *Opt. Lett.* **1994,** *19*, 317–319.

71 Nonlinear Optics of Organic Molecules and Polymers; Nalwa, H. S.; Miyata, S., Eds.; CRC Press: Boca Raton, FL, **1997.**

72 Rodríguez-Rosales, A. A.; Morales-Saavedra, O. G.; Román, C. J.; Ortega-Martínez, R. *Opt. Mater.* **2008,** *31*, 350–360.